

Cation Controlled Assembly and Transformation of Mono- and Bi-Sulfite Templated Dawson-Type Polyoxotungstates

Jun Yan, De-Liang Long, Haralampos N. Miras, and Leroy Cronin*

WestCHEM, Department of Chemistry, University of Glasgow, Joseph Black Building, University Avenue, Glasgow G12 8QQ, U.K.

Received November 3, 2009

The Dawson-like polyoxometalate clusters $(\text{TEAH})_6[\text{H}_2\text{W}_{18}\text{O}_{57}(\text{SO}_3)]$ (**1**) and $(\text{DMAH})_8[\text{W}_{18}\text{O}_{56}(\text{SO}_3)_2(\text{H}_2\text{O})_2]$ (**2**) were synthesized under similar reaction conditions by employing triethanolammonium (TEAH^+) and dimethylammonium (DMAH^+) as cations, respectively. Crystallographic studies revealed that compound **1** has a compressed, peanut-like $\{\text{W}_{18}\}$ cage containing a single sulfite anion where each cage metal atom supports one terminal oxo-based ligand whereas compound **2** also has a $\{\text{W}_{18}\}$ cage, but four of the eighteen cage metal atoms support two terminal oxo-based ligands with two sulfite anions embedded in the cluster.

Introduction

Polyoxometalates (POMs) constitute a unique class of molecular metal–oxygen clusters (containing W, Mo, V, or Nb as the metal centers), which exhibit a wide variety of structural versatility as well as important catalytic, magnetic, and optical properties.^{1–3} During the past decade, a vast number of POM studies have been undertaken and hundreds of new clusters have been discovered.⁴ However, in general, it is not possible to control or manipulate the assembly or formation of POMs without a tremendous amount of prior knowledge, especially if the planned and systematic structural design or derivatization of novel POM clusters are targeted.

Usually, POMs are synthesized at low pH in aqueous solution, and these reactions can be directed by careful variation of synthetic conditions by, for example, the ratio and concentration of the reagents, pH, counter cations, and temperature. In most cases synthesis of novel POM clusters is simple and straightforward, *once* the proper reaction

conditions have been identified, but before this the process is often trial and error.⁵ In our previous work we have described a “Shrink-Wrapping” strategy in which the presence of different organo-counter cations are employed to moderate or alter the assembly process, and this has proved to be a fruitful route to the assembly of new POMs.^{6–8} This is because the new clusters are “trapped” in solution by using organic cations and hence restrict aggregation to more highly symmetrical clusters. Among the many hundreds of hetero-POM clusters reported recently, the Dawson-type $\{\text{M}_{18}\text{O}_{54}\}$, and more specifically the sulfite-based Dawson-type POMs have received much attention because of their unique electronic and structural properties.^{9–13} The use of sulfite anions as

*To whom correspondence should be addressed. Fax: +44 141 330 4888. E-mail: l.cronin@chem.gla.ac.uk, <http://www.chem.gla.ac.uk/staff/lee>, or <http://www.croninlab.com>.

(1) (a) Pope, M. T. *Heteropoly and Isopoly Oxometalates*; Springer: Berlin, 1983. (b) Müller, A.; Peters, F.; Pope, M. T.; Gatteschi, D. *Chem. Rev.* **1998**, *98* (1), 239. (c) *Polyoxometalates: From Platonic Solids to Anti-Retro Viral Activity*; Pope, M. T., Müller, A., Eds.; Kluwer Academic Publishers: Dordrecht, The Netherlands, 1994.

(2) *Chem. Rev.: Special Thematic Issue on Polyoxometalate*, **98**, **1998**.
(3) (a) Hill, C. L. *Compr. Coord. Chem.* **2003**, *4*, 679. (b) Bi, L. H.; Körtz, U. *Inorg. Chem.* **2004**, *43*(25), 7961. (c) Körtz, U.; Savelieff, M. G.; Bassil, B. S.; Dickman, M. H. *Angew. Chem., Int. Ed.* **2001**, *40*(18), 3384. (d) An, H. Y.; Wang, E. B.; Xiao, D. R.; Li, Y. G.; Su, Z. M.; Xu, L. *Angew. Chem., Int. Ed.* **2006**, *45*(6), 904. (e) Mal, S. S.; Körtz, U. *Angew. Chem., Int. Ed.* **2005**, *44*(24), 3777. (f) Pope, M. T. *Compr. Coord. Chem.* **2003**, *4*, 635.

(4) Long, D.-L.; Burkholder, E.; Cronin, L. *Chem. Soc. Rev.* **2007**, *36*(1), 105.

(5) (a) Müller, A.; Krickemeyer, E.; Meyer, J.; Bögge, H.; Peters, F.; Plass, W.; Diemann, E.; Dillinger, S.; Nonnenbruch, F.; Randerath, M.; Menke, C. *Angew. Chem., Int. Ed.* **1995**, *34*(19), 2122. (b) Körtz, U.; Pope, M. T. *Inorg. Chem.* **1994**, *33*(25), 5643. (c) Godin, B.; Chen, Y. G.; Vaissermann, J.; Ruhlmann, L.; Verdaguer, M.; Gouzerh, P. *Angew. Chem., Int. Ed.* **2005**, *44* (20), 3072. (d) Jorris, T. L.; Kozik, M.; Baker, L. C. W. *Inorg. Chem.* **1990**, *29* (22), 4584.

(6) Long, D.-L.; Kögerler, P.; Farrugia, L. J.; Cronin, L. *Angew. Chem., Int. Ed.* **2003**, *42*(35), 4180.

(7) Long, D.-L.; Abbas, H.; Kögerler, P.; Cronin, L. *J. Am. Chem. Soc.* **2004**, *126*(43), 13880.

(8) Long, D.-L.; Kögerler, P.; Parenty, A. D. C.; Fielden, J.; Cronin, L. *Angew. Chem., Int. Ed.* **2006**, *45*(29), 4798.

(9) (a) Manos, M. J.; Woollins, J. D.; Slawin, A. M. Z.; Kabanos, T. A. *Angew. Chem., Int. Ed.* **2002**, *41*(15), 2801. (b) Miras, H. N.; Raptis, R. G.; Baran, P.; Lalioti, N.; Harrison, A.; Kabanos, T. A. *C. R. Chim.* **2005**, No. 8, 957.

(10) (a) Manos, M. J.; Miras, H. N.; Tangoulis, V.; Woollins, J. D.; Slawin, A. M. Z.; Kabanos, T. A. *Angew. Chem., Int. Ed.* **2003**, *42*(4), 425. (b) Miras, H. N.; Stone, D. J.; McInnes, E. J. L.; Raptis, R. G.; Baran, P.; Chilas, G. I.; Sigalas, M. P.; Kabanos, T. A.; Cronin, L. *Chem. Commun.* **2008**, 4703.

(11) Chilas, G. I.; Miras, H. N.; Manos, M. J.; Woollins, J. D.; Slawin, A. M. Z.; Stylianou, M.; Karamidas, A. D.; Kabanos, T. A. *Pure Appl. Chem.* **2005**, *77*(9), 1529.

(12) Dolbecq, A.; Lisnard, L.; Mialane, P.; Marrot, J.; Benard, M.; Rohmer, M. M.; Secheresse, F. *Inorg. Chem.* **2006**, *45*(15), 5898.

Table 1. Crystal Data and Structure Refinement Parameters for Compounds 1–3

	(1)	(2)	(3)
chemical formula	C ₃₆ H ₉₈ N ₆ O ₇₈ SW ₁₈	C ₁₆ H ₈₆ N ₈ O ₇₃ S ₂ W ₁₈	C ₈₆ H ₁₉₂ N ₈ O ₆₀ SW ₁₈
formula mass	5202.5	4932.35	5639.84
cryst syst	triclinic	monoclinic	tetragonal
space group	<i>P</i> $\bar{1}$	<i>P</i> 2(1)/ <i>m</i>	<i>I</i> 4
<i>T</i> (K)	150	150	150
<i>a</i> (Å)	13.4468(3)	13.8974(2)	41.803(2)
<i>b</i> (Å)	13.9726(4)	21.4577(3)	41.803(2)
<i>c</i> (Å)	14.3083(4)	15.9687(2)	15.7889(16)
α (deg)	63.971(1)	90	90
β (deg)	76.702(2)	92.380(1)	90
γ (deg)	82.723(2)	90	90
<i>V</i> (Å ³)	2349.88(11)	4757.86(11)	27591(3)
<i>Z</i>	1	2	8
μ (mm ⁻¹)	22.063	21.801	15.035
total data collected	9225	9510	23489
unique data	7457	6646	21981
<i>R</i> _{int}	0.0823	0.0467	0.0355
<i>R</i> ₁	0.0452	0.0408	0.0297
w <i>R</i> ₂ [<i>I</i> > 2 σ (<i>I</i>)]	0.1023	0.1084	0.0680
<i>R</i> (all data)	0.0618	0.0619	0.0333
w <i>R</i> ₂ (all data)	0.1088	0.1134	0.0693

templates is particularly interesting since they possess a stereochemically active lone-pair of electrons, which can impart redox activity associated directly with the template; also sulfite-based compounds possess non-linear optical properties as well as being good candidates as catalysts. For example the α -[Mo₁₈O₅₄(SO₃)₂]⁴⁻ adopts a compressed cage or “peanut” structure similar to that of [H₃SnW₁₈O₆₀]⁷⁻^{14b} but has two sulfites embedded within the cage such that the two sulfur centers are ~3.2 Å apart, indicative of a short non-covalent S···S interaction between the sulfites within the cluster cage.^{14a} Meanwhile, the cluster α -[W₁₈O₅₄(SO₃)₂]⁴⁻,¹⁵ which is iso-structural to α -[Mo₁₈O₅₄(SO₃)₂]⁴⁻, also contains two sulfites and presents interesting redox properties demonstrating a range of easily accessible charge states (-4/-5/-6).¹⁶ Furthermore, the development of POM building blocks that contain sulfite anions may be interesting for the development of larger, electronically active POM clusters.

Herein, we report the extension of the “Shrink-Wrapping” strategy in sulfite-based polyoxotungstates. By utilizing different organic cations within the reaction system, we were able to selectively isolate two structurally related clusters from very similar experimental conditions.

Experimental Section

General Considerations. Reagents were purchased commercially and used without further purification. FTIR spectra were run on a JASCO FTIR 410 spectrometer and analyzed using JASCO software. Details of X-ray diffraction experiments are included in the crystallographic data section.

Synthesis of (TEAH)₆[H₂W₁₈O₅₇(SO₃)] (1). Triethanolamine hydrochloride (4.0 g, 21 mmol) and Na₂WO₄·2H₂O (1.6 g, 4.8 mmol) were dissolved in water (25 mL). Hydrochloric acid

(6 M) was added dropwise under stirring, and the pH adjusted to 1.7. The addition of solid Na₂S₂O₄ (0.12 g, 0.69 mmol) resulted in a dark blue solution. The solution stirred for 3 min, filtered, and allowed to stand in air. Green needle-like crystals of **1** were collected after 2 weeks. Yield: 28% (0.4 g, 0.077 mmol). The thermogravimetry (TG) curve is shown in Supporting Information, Figure S3. In the TG curve of **1**, the continuous weight loss between 25–250 °C indicates the decomposition of the organic cations and the cluster. I.R. (KBr disk, ν /cm⁻¹): 3419, 3121, 2927, 1629, 1448, 1401, 1321, 1093, 985, 869, 761. Elemental analysis, calcd for C₃₆H₉₈N₆O₇₈SW₁₈: C 8.31, H 1.85, N1.61, Found C 8.49, H 2.13, N 1.68.

Synthesis of (DMAH)₈[W₁₈O₅₆(SO₃)₂(H₂O)₂]·9H₂O (2). Dimethylamine hydrochloride (4.0 g, 49 mmol) and Na₂WO₄·2H₂O (1.6 g, 4.8 mmol) were dissolved in water (25 mL). Hydrochloric acid (6 M) was added dropwise under stirring, and the pH adjusted to 1.7. Addition of solid Na₂S₂O₄ (0.12 g, 0.69 mmol) resulted in a dark blue solution. The solution stirred for 3 min, filtered, and allowed to stand undisturbed in air. Colorless block crystals of **2** were collected 1 week later. Yield: 22% (0.3 g, 0.061 mmol). TG data from **2** shows weight loss between 30 and 100 °C. The weight loss of 6.7% corresponds to the loss of lattice and coordinated water molecules, in good agreement with the theoretical value (calcd 6.6%). I.R. (KBr disk, ν /cm⁻¹): 3455, 3158, 2784, 2441, 1619, 1465, 1017, 950, 808. Elemental analysis, calcd for C₁₆H₈₆N₈O₇₃S₂W₁₈: C 3.90, H 1.76, N 2.27, Found C 4.03, H 1.88, N 2.40.

Synthesis of (TBA)₅[H₃W₁₈O₅₇(SO₃)]·3CH₃CN (3). (TEAH)₆[H₂W₁₈O₅₇(SO₃)] (0.1 g, 0.02 mmol) was dissolved in water (10 mL). Tetrabutylammonium bromide (1.0 g 3.5 mmol) dissolved in water (20 mL) and was added to the previous solution under stirring. The precipitate was centrifuged and washed with water, ethanol, and diethyl ether and then dried in vacuum. The compound was purified by recrystallization from acetonitrile via slow evaporation. Light-yellow block crystals of **3** formed in a week. Yield: 92.6% (0.1 g, 0.019 mmol). I.R. (KBr disk, ν /cm⁻¹): 3487, 2961, 2933, 2873, 1482, 1381, 969, 916, 879, 780. Elemental analysis, calcd for C₈₆H₁₉₂N₈O₆₀SW₁₈: C 18.3, H 3.43, N 1.99, Found C 17.73, H 3.56, N 1.42. CSI-MS, *m/z*: 2386.2, 2515.8, 2635.9, 3001.4, and 3920.8.

Synthesis of (TBA)₄[W₁₈O₅₄(SO₃)₂] (4). (DMAH)₈[W₁₈O₅₆(SO₃)₂(H₂O)₂]·9H₂O (0.1 g, 0.02 mmol) was dissolved in water (10 mL). Tetrabutylammonium bromide (1.0 g 3.5 mmol) dissolved in water (20 mL) was added to the previous solution under stirring. The precipitate was centrifuged and washed with water, ethanol, and diethyl ether and then dried under vacuum.

(13) (a) Matsumoto, K. Y.; Kato, M.; Sasaki, Y. *Bull. Chem. Soc. Jpn* **1976**, *49*(1), 106. (b) Long, D.-L.; Song, Y.-F.; Wilson, E. F.; Kögerler, P.; Guo, S.-X.; Bond, A. M.; Hargreaves, J. S. J.; Cronin, L. *Angew. Chem., Int. Ed.* **2008**, *47*, 4384.

(14) (a) Long, D.-L.; Kögerler, P.; Cronin, L. *Angew. Chem., Int. Ed.* **2004**, *43*(14), 1817. (b) Krebs, B.; Droste, E.; Piepenbrink, M.; Vollmer, G. *C.R. Acad. Sci. Paris, T. 1, Serie II* **2000**, No. 3, 205.

(15) Long, D.-L.; Abbas, H.; Kögerler, P.; Cronin, L. *Angew. Chem, Int. Ed.* **2005**, *44*(22), 3415.

(16) Fay, N.; Bond, A. M.; Baffert, C.; Boas, J. F.; Pilbrow, J. R.; Long, D.-L.; Cronin, L. *Inorg. Chem.* **2007**, *46*(9), 3502.

The compound was purified by recrystallization from acetonitrile via slow evaporation. Yield: 74% (0.08 g, 0.018 mmol). The purity of the single crystal was verified according to the literature.¹⁵ CSI-MS, m/z : 1525.1, 2408.9, 2894.3, and 5545.4.

X-ray Crystallography. Suitable single crystals were selected and mounted onto the end of a thin glass fiber using Fomblin oil. X-ray diffraction intensity data were measured at 150(2) K on a Bruker Nonius Kappa CCD or a Oxford Diffraction Gemini diffractometer [$\lambda(\text{Mo-K}\alpha) = 0.7107 \text{ \AA}$]. Structure solution and refinement were carried out with SHELXS-97 and SHELXS-97 via WinGX.¹⁷ Corrections for incident and diffracted beam absorption effects were applied using analytical methods (Table 1).¹⁸

Thermogravimetric Analysis. Thermogravimetric analysis (TGA) was performed under N_2 atmosphere at a heating rate of $15 \text{ }^\circ\text{C min}^{-1}$ on crystalline samples.

Cryospray Mass Spectroscopic Measurements. Cryospray ionization (CSI) measurements were carried out at $20 \text{ }^\circ\text{C}$. The solution of the sample was diluted so the maximum concentration of the cluster ions was of the order of 10^{-5} M , and this was infused at a flow rate of $180 \text{ }\mu\text{L/h}$. The mass spectrometer used for the measurements was Bruker micro TOF-Q, and the data were collected in both positive and negative mode. The spectrometer was previously calibrated with the standard tune mix to give a precision of about 1.5 ppm in the region of 500–5000 m/z . The standard parameters for a medium mass data acquisition were used, and the end plate voltage was set to -500 V and the capillary to $+4500 \text{ V}$. The collision cell was set to collision energy to -8.0 eV/z with a gas flow rate at 25% of maximum, and the cell RF was set at 600 Vpp.

Electrochemistry. Voltammograms were obtained using a Model Versastat 4 electro analysis system by Princeton Applied Research. The standard three-electrode arrangement was employed with a Pt mesh auxiliary electrode, 1.5 mm glassy carbon working electrode, and Ag/AgCl reference electrode. All potentials are quoted relative to the Ag/AgCl reference electrode. The glassy carbon working electrodes (diameter 1.5 mm) were polished with alumina ($3 \text{ }\mu\text{m}$) on polishing pads, rinsed with distilled water, and sonicated in H_2O and then acetone solution before each experiment. Doubly distilled water was used to prepare all aqueous solutions. For electrochemical studies, dioxygen was removed by purging aqueous solutions with argon for at least 10 min. Na_2SO_4 was used as electrolyte. The 0.1 M acetate buffer system was prepared by adding 2.4 mL of a 0.1 M sodium acetate solution to 7.6 mL of a 0.1 M acetic acid solution ($\text{pH} = 4.2$). The required amount of solid Na_2SO_4 was then added (effecting a 0.20 M Na_2SO_4 solution) along with the desired amount of the compound (effecting a $2 \times 10^{-3} \text{ M}$ solution).

Results and Discussion

When triethanolammonium (TEAH^+) was used as the “shrink-wrapping” cation, the self-assembly of a new Dawson-like POM cluster, $(\text{TEAH})_6[\text{H}_2\text{W}_{18}\text{O}_{57}(\text{SO}_3)]$ (**1**), which contains only one sulfite within a cavity, was achieved. Further, when the TEA/TEAH was replaced by dimethylamine (DMA), a Dawson-like cluster, $[\text{W}_{18}\text{O}_{56}(\text{SO}_3)_2(\text{H}_2\text{O})_2]^{8-}$, this time containing two sulfites within the cavity is found. Although this cluster is structurally identical to a “Trojan Horse” type-cluster we reported previously,¹⁵ this cluster was obtained as the organic soluble dimethylammonium salt, $(\text{DMAH})_8[\text{W}_{18}\text{O}_{56}(\text{SO}_3)_2(\text{H}_2\text{O})_2] \cdot 9\text{H}_2\text{O}$ (**2**).

(17) (a) Sheldrick, G. M. *Direct Methods Solving Macromol. Struct.* **1998**, 507, 401. (b) Sheldrick, G. M. *Direct Methods Solving Macromol. Struct.* **1998**, 507, 131. (c) Sheldrick, G. M. *Direct Methods Solving Macromol. Struct.* **1998**, 507, 119.

(18) Blessing, R. H. *Acta Crystallogr., Sect. A* **1995**, 51, 33.

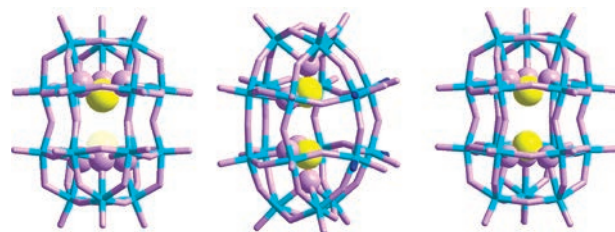
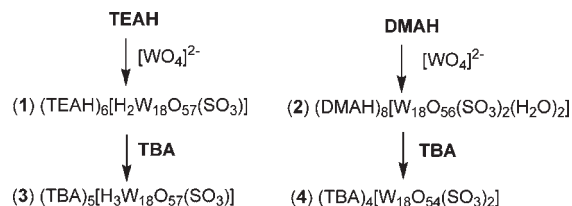


Figure 1. Representations of the structures of the cluster anions found in compounds **1** and **2**: β - $[\text{H}_2\text{W}_{18}\text{O}_{57}(\text{SO}_3)]^{6-}$ (left), **3**: $[\text{W}_{18}\text{O}_{56}(\text{SO}_3)_2(\text{H}_2\text{O})_2]^{8-}$ (middle) and **4**: α - $[\text{W}_{18}\text{O}_{54}(\text{SO}_3)_2]^{4-}$ (right) cluster anions. S atoms shown in yellow spheres, O and W centres in pink and cyan sticks respectively.

Scheme 1. Assembly of Compounds **1** and **2** in the Presence of TEAH and DMAH, Respectively, and Ion Exchange of Compounds **1** and **2** to **3** and **4**, Respectively^a



^aAlso, the ion exchange of compound **2** results in a structural re-arrangement of the cluster architecture to cluster **4**.

What is perhaps most intriguing is that the cations of compound **1** (TEAH) can be exchanged for TBA to give $(\text{TBA})_5[\text{H}_3\text{W}_{18}\text{O}_{57}(\text{SO}_3)] \cdot 3\text{CH}_3\text{CN}$, compound (**3**), yet a similar ion exchange reaction of compound (**2**), results in the reorganization of the cluster to compound (**4**), $(\text{TBA})_4[\text{W}_{18}\text{O}_{54}(\text{SO}_3)_2]$, see Scheme 1 and Figure 1.

In the presence of triethanolammonium, compound **1** ($(\text{TEAH})_6[\text{H}_2\text{W}_{18}\text{O}_{57}(\text{SO}_3)]$), was obtained from the reaction of tungstate with dithionite which in turn produces the sulphite anions. Notably, a similar reaction system, in the absence of reducing agent, yields the cluster $[\text{H}_{12}\text{W}_{36}\text{O}_{120}]^{12-}$ but the role of the reducing agent is not really understood since the resulting cluster is fully oxidized.^{7,19} It is interesting that compound **2** was synthesized under similar experimental conditions using dimethylammonium instead of TEAH^+ , and that the compound includes two sulfite ions even though the concentration of sulfite is not a limiting factor. Further, the cation symmetry appears, as we suggested previously,^{4,6} to correlate with the symmetry of the cluster anion. Although this hypothesis is not yet fully testable, the cation triethanolammonium, which has a 3-fold symmetry, has been shown to be experimentally essential to isolate the 3-fold symmetric β - $[\text{H}_2\text{W}_{18}\text{O}_{57}(\text{SO}_3)]^{6-}$. It is interesting that the use of dimethylammonium, with 2-fold symmetry, gives rise to the assembly of the 2-fold symmetric cluster $[\text{W}_{18}\text{O}_{56}(\text{SO}_3)_2(\text{H}_2\text{O})_2]^{8-}$. These are further observations, based upon weakly correlated circumstantial observations that there may be a correlation between the charge balancing cation symmetry and the symmetry of the cluster isolated. We have proposed this before;^{4,6} however, this hypothesis needs far more data, but nevertheless is an interesting observation.

The cluster β - $[\text{H}_2\text{W}_{18}\text{O}_{57}(\text{SO}_3)]^{6-}$ found in **1** has an overall peanut-like shape (where the cigar-shaped cluster is pinched,

(19) Long, D.-L.; Brucher, O.; Streb, C.; Cronin, L. *Dalton Trans.* **2006**, No. 23, 2852.

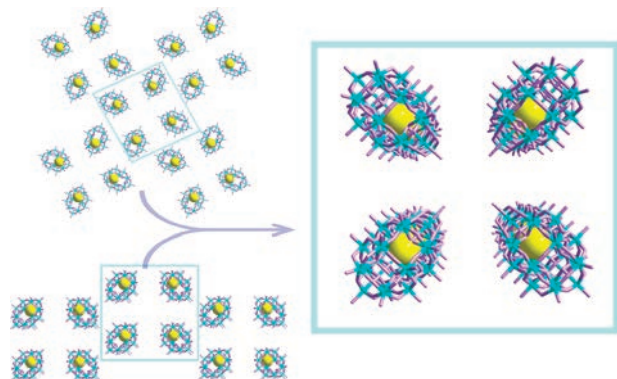


Figure 2. Representations of the packing mode of **1**: β -[H₂W₁₈O₅₇(SO₃)⁶⁻]. **Above**: view along the 4-fold axis; **below**: side view of the 4-fold axis showing polar packing of the cluster. The {W₁₈} cage is shown in wire mode and each cyan line represents one W center. The S atoms are shown by the yellow spheres and the O ligands are depicted by the pink colored sticks.

or compressed at the equator to give two lobes), which has a pseudosymmetric center and overall approximate D_{3d} symmetry and incorporates the pyramidal sulfite ion (SO₃²⁻) ion as the central cluster template. As shown in Figure 1, the {W₁₈} Dawson framework consists of two equivalent B–W₉O₃₃ half units that have C_{3v} symmetry, and the two parts are linked to each other by sharing six oxygen atoms and form a D_{3d} {W₁₈O₅₄} framework. The single S atom from the sulfite moiety is disordered over the two possible sites separated by a distance of 3.0 Å from each other with a sulfur occupancy being 0.5 on each site. Unlike the α -[W₁₈O₅₄(SO₃)₂]⁴⁻, which has a crystallographic mirror plane normal to the axis containing the two sulfites,¹⁹ there is an inversion center located between the two sulfite sites in β -[H₂W₁₈O₅₇(SO₃)⁶⁻]. As such, it is interesting to note that the “real” sulfur position significantly shifts toward the cluster center, resulting in a much longer average S–O distance (~1.69 Å). Compared with those in α -[W₁₈O₅₄(SO₃)₂]⁴⁻,¹⁵ the S–O distances in **1** are enlarged by ~0.15 Å and the S···S(virtual) distance is shortened by ~0.3 Å.

The situation of the monosulfite templation in **1** is somewhat different from the non-classical Dawson clusters ({W₁₈}) hosting single pyramidal group (AsO₃³⁻, SbO₃³⁻, BiO₃³⁻, or TeO₃²⁻).²⁰ It is hypothesized that in these clusters the {W₁₈} cage can only incorporate one heteroatom because of their large ionic radii which results in steric crowding physically preventing the inclusion of two units in the clusters. For example, the Te···Te(virtual) distance in [H₃W₁₈O₅₇(TeO₃)³⁻] is only 2.2 Å, far smaller than the sum of the radii of two Te atoms thereby disfavoring the formation of a {W₁₈} cluster that includes two Te-based templates. However the α -[W₁₈O₅₄(SO₃)₂]⁴⁻, on the other hand, is stable and can be found with two sulfur atoms as reported previously.¹⁵ This observation suggests, in the case of the reaction system that produces the monosulfite compound **1**, that steric factors do not prevent the formation of the bisulfite, that is, the size of the sulfur is not the key factor in favoring one or two hetero anion templation. It is also interesting that the cluster crystallized in the I_4 chiral space group as TBA⁺ salt when it is transferred to the organic phase.



Figure 3. Comparison of the {W₉} half in **1**: [H₂W₁₈O₅₇(SO₃)⁶⁻] (left), **2**: [W₁₈O₅₆(SO₃)₂(H₂O)₂]⁸⁻ (middle) and [W₁₈O₅₄(SO₄)₂]⁴⁻ (right). Yellow spheres: S; pink spheres: O. The {W₉} cage is shown in wire mode. Each cyan line represents one {W₆} part, and the disorder coordinated water positions are highlighted in blue.

As shown in Figure 2, the two disordered positions are not equal in the cluster with occupancy ratio of 0.6:0.4, and the clusters pack in “head to head” arrangement within the crystal structure. This means the “real” and “empty” sulfur sites are partially resolved in the crystalline state. This is interesting and implies that there is some electrostatic stabilization that favors the head-to-head packing motif where the sulfite ion is shown to occupy the head space.

When TEA is replaced by dimethylamine (DMA), that is, where the only variable that is changed is the amine, compound **1** no longer forms, but instead compound **2**, the “Trojan Horse” cluster [W₁₈O₅₆(SO₃)₂(H₂O)₂]⁸⁻ is obtained. We have previously isolated this cluster anion as a potassium salt.¹⁵ However, it was difficult to examine the aqueous chemistry of the product due to solubility issues. As shown in Figure 3, the structure of the cluster consists of two {W₉(SO₃)} halves which contain six equatorial and three capping metal positions. The two halves are joined together via six μ_3 -oxo ligands which ligate to the six equatorial metal positions on each {W₉(SO₃)} fragment.

The SO₃ pyramids are tilted so that only seven of the nine metal centers of each {W₉(SO₃)} fragment are connected, and this arrangement leaves four neighboring equatorial tungsten centers adjacent to, but not coordinated to the sulfite groups. As a result each of these four tungsten ions has two, rather than one, terminal ligands (as is found normally in Dawson-like clusters), and these extra terminal ligand positions are occupied by water or oxo ligands (two terminal oxo and two waters disordered over the four positions). In addition, the orientation of the sulfite also reduces the overall molecular symmetry to be C_{2v} with the loss of the C_3 axis found in compound **1**.

The different orientations of the sulfite ions leads to an increase of the S···S distance to 3.61(2) Å while the average S–O distance is 1.55 Å. Importantly, the structure is very similar to the traditional Dawson cluster α -[W₁₈O₅₄(SO₄)₂]⁴⁻. Indeed an overlay of the metal and S positions in the sulfate structure compared with the cluster anion in compound **2** shows that these positions are virtually identical. The only difference is one sulfate bridging oxygen is missing, and the presence of the water molecules.

The synthesis of these compounds reveals interesting facts about the role of the cations in the formation of the clusters. This is because the organic cations appear to have a role as external structure directing “templates” and significantly affect the assembly process; that is, the geometry of the organo-cations can guide the formation of differing clusters. The C_{3v} symmetric TEAH⁺ cation guides the formation of C_{3v} {SW₉O₃₃} fragment and the cluster [H₂W₁₈O₅₇(SO₃)⁶⁻] in D_{3d} symmetry, while the C_{2v} symmetric DMA cation guides the formation of the {SW₉O₃₅} fragment of C_s

(20) (a) Jeannin, Y.; Martinfrere, J. *Inorg. Chem.* **1979**, *18*(11), 3010. (b) Ozawa, Y.; Sasaki, Y. *Chem. Lett.* **1987**, No. 5, 923. (c) Wang, J. P.; Ma, P. T.; Zhao, J. W.; Niu, J. Y. *Inorg. Chem. Commun.* **2007**, *10*(5), 523. (d) Yan, J.; Long, D.-L.; Wilson, E. F.; Cronin, L. *Angew. Chem., Int. Ed.* **2009**, *48*(24), 4376.

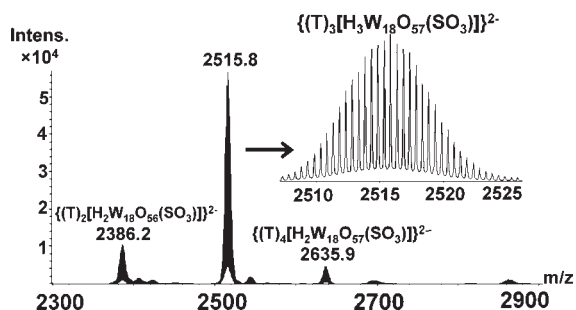


Figure 4. Negative ion mode Mass spectra of $(\text{TBA})_3[\text{H}_3\text{W}_{18}\text{O}_{57}(\text{SO}_3)]^{2-}$ **3** in acetonitrile ($\text{T} \equiv \text{TBA}^+$).

symmetry, and then the cluster $[\text{W}_{18}\text{O}_{56}(\text{SO}_3)_2(\text{H}_2\text{O})_2]^{8-}$ in C_{2v} symmetry.

Because of the long S–O bond distances and the disorder of the heteroanion in **1**, it is challenging to identify the central atoms simply from X-ray crystallography. To confirm the identity of the central heteroatom template, high-resolution cryospray mass spectrometry study was employed to investigate the compounds.^{21,22} In these experiments, the TEAH and DMAH cations were replaced by TBA since this should aid the separation because of the higher molecular weight of TBA^+ compared to TEAH and DMAH; this will give a larger separation between signals corresponding to differently charged or protonated cluster states. Second, the use of TBA salts means that acetonitrile can be employed as a solvent, which can be favorable to prevent decomposition or respeciation of the clusters which is typically observed in aqueous solution.

The ESI-MS study of compound **3** (resulting from the ion exchange of compound **1**) in acetonitrile shows that the expected monosulfite $\{\text{W}_{18}\text{S}\}$ cluster anion is present and all the main peaks can be assigned to different charge/cation states of this (see the Supporting Information): m/z 2515.8 $\{(\text{TBA})_3[\text{H}_3\text{W}_{18}\text{SO}_{60}]\}^{2-}$, 3434.8 $\{(\text{TBA})_7[\text{H}_3\text{W}_{18}\text{SO}_{60}]\}^{3-}$, 3001.4 $\{(\text{TBA})_7[\text{H}_3\text{W}_{18}\text{SO}_{60}]\}^{2+}$, see Figure 4 for the spectrum including an expansion of the main peak in negative mode.

The ESI-MS experiment with ion compound **3** clearly shows that the cluster is 3-fold protonated compared to the doubly protonated species found in compound **1**; however, the composition of the main framework is otherwise identical as expected. It is interesting also to observe that the cluster is labile and that the parent 3-fold protonated cluster can decompose via water loss, as this is indicated by the peak at 2386.2; this can be assigned to the $\{(\text{TBA})_2[\text{H}_2\text{W}_{18}\text{O}_{56}(\text{SO}_3)]\}^{2-}$ species which indicates that the decomposition process of the 3-fold protonated cluster may begin with the loss of one water molecule. In contrast, the ESI-MS spectra of the cluster anion found in **4** in acetonitrile solvent are also recorded, and the expanded main peak is represented in Figure 5, which gives totally different results. As reported before,¹⁵ the $[\text{W}_{18}\text{O}_{56}(\text{SO}_3)_2(\text{H}_2\text{O})_2]^{8-}$ cluster rearranges during the cation exchange process and forms the $[\text{W}_{18}\text{O}_{54}(\text{SO}_3)_2]^{4-}$ cluster. All the main peaks can be assigned related to $\{\text{W}_{18}\text{S}_2\}$: m/z 2408.9 $\{(\text{TBA})_2[\text{W}_{18}\text{O}_{54}(\text{SO}_3)_2]\}^{2-}$, 2894.3 $\{(\text{TBA})_6[\text{W}_{18}\text{O}_{54}(\text{SO}_3)_2]\}^{2+}$. Unlike the spectrum of

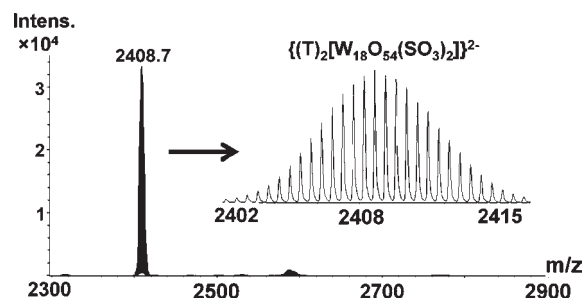


Figure 5. Negative ion mode Mass spectra of $(\text{TBA})_4[\text{W}_{18}\text{O}_{54}(\text{SO}_3)_2]^{2-}$ **4** in acetonitrile. ($\text{T} \equiv \text{TBA}^+$).

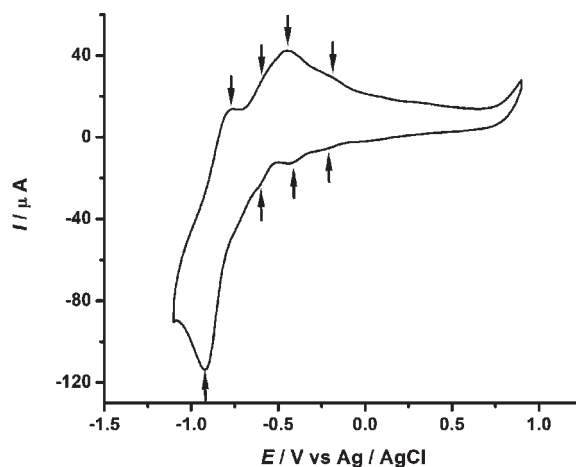


Figure 6. Cyclic voltammograms of **1** (2×10^{-3} M) in aqueous 0.2 M Na_2SO_4 of 1 M $\text{CH}_3\text{COOH}/\text{CH}_3\text{COONa}$ buffer solution ($\text{pH} = 4.2$). The scan rate was 100 mV s^{-1} , the working electrode was glassy carbon (1.5 mm), and the reference electrode was Ag/AgCl .

compound **3**, there is no observation of a protonated cluster or fragment peaks at the same conditions. Therefore, evidence from MS spectral studies, in combination with elemental analysis, crystallography, IR, and TGA, clearly show that compound **3** and compound **4** contain one and two sulfite anions inside the clusters, respectively.

The redox behavior of the compounds **1** and **2** were studied in buffered aqueous solution. Figure 6 shows the main characteristic peaks associated with W centered redox couples of compound **1** in the region -0.900 to $+1.000$ V of potential values versus Ag/AgCl at a scan rate of 100 and 25 mV s^{-1} . The form of the diagram remained identical independent of the scanning potential direction, indicating that the phenomena observed in one domain had a negligible influence on those in the other domain. At the aforementioned scan rate and scanning toward the negative region of potential values, the reduction of W centers for compound **1** occurs through three overlapping quasi-reversible (vs Ag/AgCl) redox couples, with the corresponding $E_{1/2}$ peak potentials located respectively at -0.214 , -0.442 , and -0.586 V while a consecutive fourth quasi-reversible process is located at $E_{1/2} = -0.846$.

In the case of compound **2** were observed four quasi-reversible redox processes located at $E_{1/2}$ peak potentials of -0.050 , -0.273 , -0.469 , and -0.603 V, respectively, as shown in Figure 7. Interestingly, in the region of positive potentials for compound **2** we observed two electrochemically irreversible oxidations of the encapsulated sulfite to sulfate anions. To exclude any possible redox process from the DMA molecules, we repeated the CV under the same

(21) (a) Long, D.-L.; Streb, C.; Song, Y.; Mitchell, S.; Cronin, L. *J. Am. Chem. Soc.* **2008**, *130*, 1830. (b) Pradeep, C.; Long, D.-L.; Kögerler, P.; Cronin, L. *Chem. Commun.* **2008**, 4254. (c) Miras, H. N.; Wilson, E.; Cronin, L. *Chem. Commun.* **2009**, 1297.

(22) Wilson, E.; Abbas, H.; Duncombe, B.; Streb, C.; Long, D.-L.; Cronin, L. *J. Am. Chem. Soc.* **2008**, *130*, 13876.

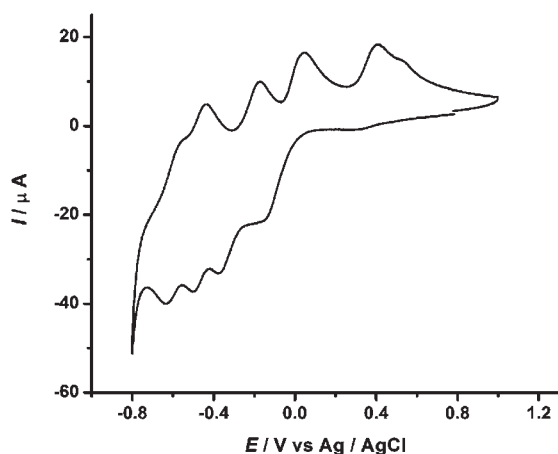


Figure 7. Cyclic voltammogram of compound **2** (2×10^{-3} M) in aqueous 0.2 M Na_2SO_4 of 1 M $\text{CH}_3\text{COOH}/\text{CH}_3\text{COONa}$ buffer solution (pH = 4.2). The scan rate was 100 mV s^{-1} , the working electrode was glassy carbon (1.5 mm), and the reference electrode was Ag/AgCl.

conditions in the absence of the POM molecule where no redox process has been observed. The striking differences in orientation between the sulfite anions in the clusters found in compounds **1** and **2** are therefore nicely demonstrated by the electrochemical investigations whereby no oxidation processes are observed for the sulfite anions present in compound **1**. This is not unexpected since the cluster found in compound **2** is perfectly set up for the oxidation process; not only do four of the 18 tungsten atoms have two terminal ligands but also the reorganization of the framework oxygen atoms results in the oxidation of the sulfite to sulfate commensurate with the loss of two water ligands. Whereas in compound **1**, there are no available leaving groups and the sulfite anions are in the wrong orientation for oxidation within the cavity of the cluster. Furthermore, the cyclic voltammograms of both compounds at different scan rates are measured (see Supporting Information). The peak height was proportional to both the concentration and the square root of scan rate under these conditions, confirming ideal diffusion-controlled behavior in the 25–400 mV/s region of scan rate. As was expected, the observed voltammogram pattern of compound **2** is similar to the corresponding one for the $\{\text{Mo}_{18}(\text{SO}_3)_2\}$ cage. Even though the two cages represent Dawson structural motifs, the aforementioned redox coupling pattern of compound **2** redox couples is shifted toward more negative potential values since the tungsten centers are harder to reduce as well as the effective negative charge on the cage is reduced in the case of the Mo-analogue which incorporates 54 oxygen atoms instead of 56.²³ Also, the characteristics of the W-waves depend on the pH and on the buffering strength of the electrolyte,

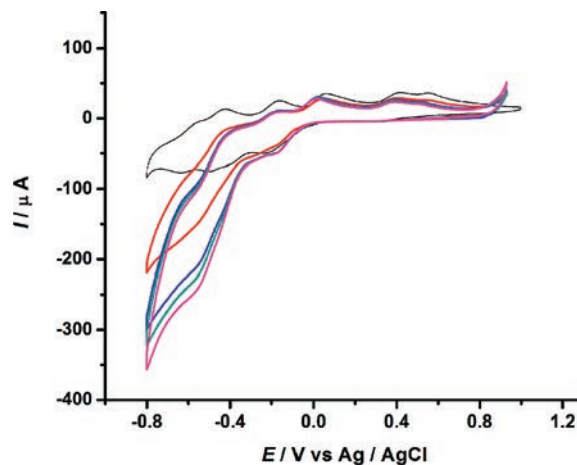


Figure 8. CVs of compound **2** addressing just the first redox processes of the W centers, in the absence of NO_2^- (dotted line), and after addition of specific amount of NO_2^- ; $C = 5, 7, 10,$ or 12 mM .

and this is a well-known electrochemical behavior for the majority of the POMs.^{24–27}

Interestingly, the redox potential values for the monosulfite species are shifted toward more negative potential values in comparison to the bisulfite analogue. Upon first inspection this would seem to be in contrast to the electronic structure of the two compounds since, upon increasing the electron density within the cluster shell from the lone pairs formally associated with each SO_3 group, one would expect the $\{\text{W}_{18}(\text{SO}_3)_2\}$ to be harder to reduce since this effect is felt by the metal framework thereby shifting the potentials toward more negative values. However the structures of the two compounds differ in terms of the number of incorporated oxygen/oxo ligands in the cages, and compound **2** actually has fewer oxygen/oxo ligands attached (56 vs 57) which would explain this trend (The cage's charge is effectively the same in both cases, 8–, since compound **1** is 2-fold protonated).

The associated catalytic activities of these polyanions toward the reduction of NO_2 also have been investigated. The direct electro-reduction of NO_2 requires in general a large overpotential.²⁸ The previous reported work has demonstrated the quantitative conversion of NO into N_2O by a selection of one- and two-electron reduced POMs.²⁹ In the present case, accumulation of electrons in the POM framework as observed with compounds **1** and **2** is, thus, likely to produce highly reduced nitrogen compounds if such a system could act catalytically against the series of NO_x species.³⁰ Upon addition of NO_2^- in the same medium for compound **2**, the cathodic current of the second and third wave respectively is enhanced remarkably, while the corresponding anodic current nearly disappears, as shown in Figure 8. This observation is indicative of electrocatalytic behavior against NO_2 . It is worth noting at this point that compound **2** shows large electrocatalytic effect in contrast to compound **1** which does not show any appreciable activity.

(23) Baffert, C.; Feldberg, S. W.; Bond, A. M.; Long, D.-L.; Cronin, L. *Dalton Trans.* **2007**, 4599.

(24) Bi, L. H.; Wang, E.-B.; Peng, J.; Huang, R. D.; Xu, L.; Hu, C. W. *Inorg. Chem.* **2000**, 39(4), 671.

(25) Mbomekalle, M.; Keita, B.; Nadjo, L.; Berthet, P.; Neiwert, W. A.; Hill, C. L.; Ritorto, M. D.; Anderson, T. M. *Dalton Trans.* **2003**, 2646.

(26) (a) Liw, J.; Ortega, F.; Sethuraman, P.; Katsoulis, D. E.; Costello, C. E.; Pope, M. T. *Dalton Trans.* **1992**, 1901. (b) Mbomekalle, I. M.; Keita, B.; Nierlich, M.; Kortz, U.; Berthet, P.; Nadjo, L. *Inorg. Chem.* **2003**, 42(17), 5143. (c) Jabbour, D.; Keita, B.; Mbomekalle, I. M.; Nadjo, L.; Kortz, U. *Eur. J. Inorg. Chem.* **2004**, 2036.

(27) (a) Keita, B.; Lu, Y. W.; Nadjo, L.; Contant, R. *Eur. J. Inorg. Chem.* **2000**, 567. (b) Sadakane, M.; Steckhan, E. *Acta Chem. Scand.* **1999**, 53, 837.

(28) (a) Dong, S. J.; Xi, X. D.; Tian, M. J. *Electroanal. Chem.* **1995**, 385, 227. (b) Keita, B.; Nadjo, L. *J. Electroanal. Chem.* **1987**, 227, 77. (c) Keita, B.; Belhouari, A.; Nadjo, L.; Contant, R. *J. Electroanal. Chem.* **1988**, 247, 157.

(29) Belhouari, A.; Keita, B.; Nadjo, L.; Contant, R. *New J. Chem.* **1998**, 22, 83.

(30) Bassil, B. S.; Kortz, U.; Tigan, A. S.; Clemente-Juan, J. M.; Keita, B.; de Oliveira, P.; Nadjo, L. *Inorg. Chem.* **2005**, 44(25), 9360.

Conclusions

We have shown that the self-assembly of POM clusters can be critically controlled by the cation type, with some evidence that the symmetry of the cation and anion can be correlated. In this work we have used this observation to produce Dawson-like clusters that contain mono and disulfite anions yielding $[\text{H}_2\text{W}_{18}\text{O}_{57}(\text{SO}_3)]^{6-}$ (found in compound **1**) and $[\text{W}_{18}\text{O}_{56}(\text{SO}_3)_2(\text{H}_2\text{O})_2]^{8-}$ (found in compound **2**) from TEA and DMA, respectively. Further, ion exchange of compound **1** replacing TEA for TBA results in the same cluster being isolated whereas ion exchange of compound **2** results in $[\text{W}_{18}\text{O}_{54}(\text{SO}_3)_2]^{4-}$ being isolated in compound **4**. Thus, the anion found in compound **4** represents the structural equivalent of the anion found in compound **1**, but now containing two sulfite anions. The monosulfite system can crystallize in such a way to promote the head-to-head assembly of the clusters whereby the central disordered sulfite tends to occupy the headspace. Not only were these clusters crystallographically and analytically studied, electrospray mass spectrometry studies revealed the sulfite content, the extent of the protonation, as well as the stability of the structural motif in solution. Moreover, electrochemical studies showed an interesting conversion of the $\{\text{W}_{18}(\text{SO}_3)_2\}$ cage to the $\{\text{W}_{18}(\text{SO}_4)_2\}$ in solution through an electrochemical oxidation. Furthermore, this has been demonstrated through the above-mentioned process: the ability of the

“Trojan horse” architecture to react according to the environmental redox conditions. On the contrary, the monosulfite analogue showed no reactivity, since the rigidity of the cage in this case does not facilitate the oxidation of the trapped heteroanion to take place through a structurally confined electron transfer process. Additionally, compound **2** showed electrocatalytic properties with nitrite substrates; this shows that the compound has not only the ability to store electrons, but also in electron transfer reactions with potential catalytic applications. All these observations mean that these clusters have tremendous potential for the development of new catalysts, electronic materials, and devices. In further work we will try and expand our studies with respect to using the organo-cations to control the assembly of the cluster anions to reach the elusive stage whereby we can assemble almost any Dawson-cluster guest combination as a function of the counterion employed.

Acknowledgment. We thank the EPSRC, the Chinese Scholarship Council, WestCHEM, and the University of Glasgow for supporting this work. L.C. thanks the Royal Society & Wolfson Foundation for a merit award.

Supporting Information Available: The CSI-MS spectrum details, cyclic voltammogram results, and TGA data. This material is available free of charge via the Internet at <http://pubs.acs.org>.